RSC Advances

PAPER

View Article Online
View Journal | View Issue

Cite this: *RSC Adv.*, 2022, **12**, 6076

Hydrogen-bond super-amphiphile based drug delivery system: design, synthesis, and biological evaluation†

Jiali Chen,[a] Haolong Huang,[b] Ruilin Lu,[b] Xiaohui Wan,[a] Yongchao Yao,[b] Tian Yang,[b] Pengfei Li,*[b] Ning Ning[a] and Shiyong Zhang*[b]

Received 25th November 2021
Accepted 25th January 2022

DOI: 10.1039/d1ra08624c

rsc.li/rsc-advances

Drug delivery systems (DDSs) show great application prospects in tumor therapy. So far, physical encapsulation and covalent grafting were the two most common strategies for the construction of DDSs. However, physical encapsulation-based DDSs usually suffered from low drug loading capacity and poor stability, and covalent grafting-based DDSs might reduce the activity of original drug, which greatly limited their clinical application. Therefore, it is of great research value to design a new DDS with high drug loading capacity, robust stability, and original drug activity. Herein, we report a super-amphiphile based drug delivery system (HBS-DDS) through self-assembly induced by hydrogen bonds between amino-substituted N-heterocycles of the 1,3,5-triazines and hydrophilic carmofur (HCFU). The resulting HBS-DDS had a high drug loading capacity (38.1%) and robust stability. In addition, the drug delivery system exhibited pH-triggered size change and release of drugs because of the pH responsiveness of hydrogen bonds. In particular, the anticancer ability test showed that the HBS-DDS could be efficiently ingested by tumor cells, and its half-maximal inhibitory concentration (IC_{50} = 3.53 μg mL^{-1}) for HeLa cells was close to that of free HCFU (IC_{50} = 5.54 μg mL^{-1}). The hydrogen bond-based DDS represents a potential drug delivery system in tumor therapy.

1. Introduction

Drug delivery systems (DDSs) have shown great application prospects in tumor therapy due to their long blood half-life and enhanced permeability and retention (EPR) effect.[1–3] So far, physical encapsulation and covalent grafting were currently the two most common strategies for the construction of DDS. As reported, physical encapsulation could effectively maintain the efficacy of original drug, but it usually had the following two disadvantages: (1) low drug loading capacity (usually <5%) caused the use of a large number of nontherapeutic carrier materials; (2) poor stability might lead to drug molecule leakage.[4–7] In contrast, covalent grafting could significantly improve the drug loading efficiency and stability of DDS.[4,8] Nevertheless, covalent grafting sometimes need to occupy the functional groups of drugs and affects the release of drugs in the lesion, which would reduce or even change the activity of original drugs.[9,10] Thus, it is still a hotspot and challenge in the field of tumor therapy to find a general strategy to build a DDS with high drug loading capacity, robust stability, and original drug activity.

Recently, loading based on non-covalent interactions, provided a new idea to solve the above problems, as it could not only retain the advantages of physical encapsulation and covalent grafting but also overcome their disadvantages.[11–13] For example, our groups reported a DDS based on electrostatic interaction, which not only exhibited a high drug loading content (up to 45.0%) and robust stability but also maintained the activity of loaded chemotherapeutic drugs.[10] As non-covalent interactions, hydrogen bonding was also widely used in the design and construction of DDS. A large number of studies have demonstrated that the drug loading system based on hydrogen bonds not only had high drug loading capacity and excellent stability but also could intelligently release loaded drugs due to the pH responsiveness of hydrogen bonds.[14–16]

Herein, we reported a new hydrogen-bond super-amphiphile-based drug delivery system (HBS-DDS) for tumor therapy. As shown in Scheme 1, the HBS-DDS was constructed through self-assembly induced by hydrogen bonds between carrier molecules (amino-substituted N-heterocycles of the 1,3,5-triazines, **1**) and anticancer drugs (hydrophilic carmofur, HCFU). The hydrogen bond between carriers and drugs endowed the HBS-DDS with high drug loading capacity and

[a]*West China School of Nursing/West China Hospital Orthopedics Department, Sichuan University, 37 Guo Xue Xiang, Chengdu 610041, China*

[b]*College of Biomedical Engineering and National Engineering Research Center for Biomaterials, Sichuan University, 29 Wangjiang Road, Chengdu 610064, China. E-mail: lipengfei0604@163.com; szhang@scu.edu.cn; Fax: +86-28-85411109; Tel: +86-28-85411109*

† Electronic supplementary information (ESI) available. See DOI: 10.1039/d1ra08624c

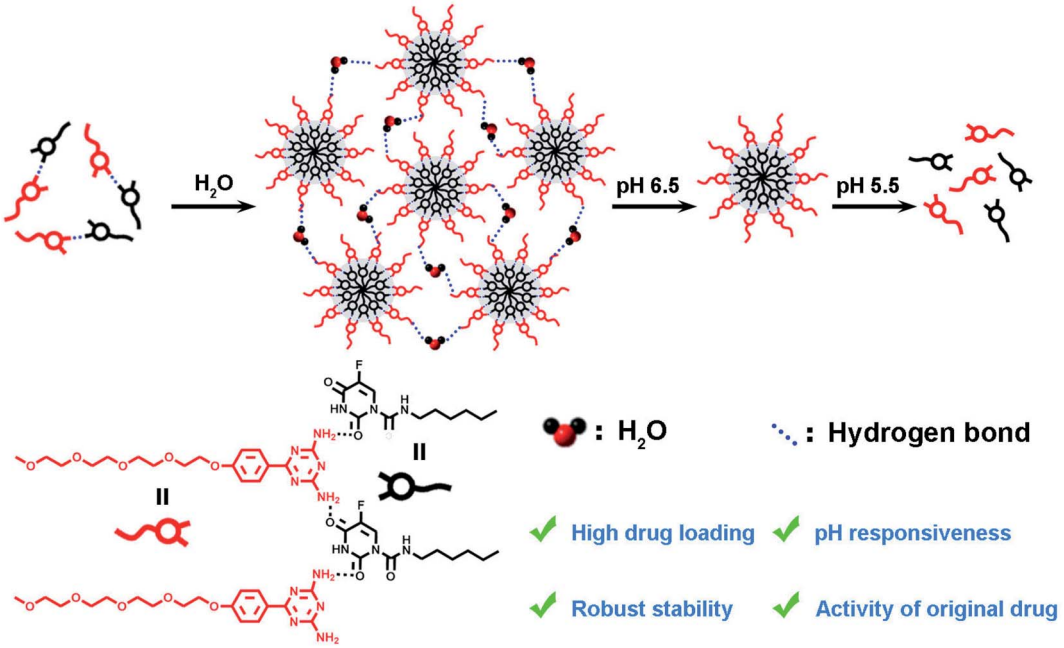

Scheme 1 Preparation of the hydrogen-bond super-amphiphile-based drug delivery system.

robust stability. Owing to the pH sensitivity of hydrogen bonds, the HBS-DDS exhibited pH-triggered size change and drug release behavior. The anticancer ability test showed that HBS-DDS could not only be efficiently ingested by tumor cells but also its anticancer activity was close to that of HCFU. Thus, HBS-DDS with high drug loading capacity, robust stability, original drug activity, and pH responsiveness would be a potential nano-drug for clinical tumor treatment.

2. Experimental section

2.1 Material

Sodium hydroxide, potassium hydroxide, dinitrile diamine, anhydrous acetone, petroleum ether, ethyl acetate, dichloromethane, anhydrous potassium carbonate, dimethyl sulfoxide, Tween 80, and hydrochloric acid *p*-toluenesulfonyl chloride were purchased from Chengdu Chron Chemicals Co. Ltd, China. Tetraethylene glycol monomethyl ether, 4-hydroxybenzonitrile, diethylene glycol methyl ether, and hydrophobic carmofur (HCFU) were purchased from Tansoole (Shanghai, China). The dialysis bag was purchased from Spectrum Laboratories, Inc. USA. DMEM culture medium, fetal bovine serum (FBS), and pancreatin were purchased from Cytiva HyClone Laboratories, USA. Paraformaldehyde was purchased from Tianjin ZhiYuan Reagent Co. Ltd, China. Hoechst 33342 cell was purchased from Merck Sigma-Aldrich, USA. Counting kit-8 (CCK-8) was purchased from Beyotime Biotech Inc., China.

2.2 Preparation of HBS-DDS

Compound **1** (amino-substituted N-heterocycles of the 1,3,5-triazines, 3.9 mg, 0.01 mmol) was dissolved in dimethyl sulfoxide (100 mL; DMSO). Then, the ultra-pure (UP) water (4 mL) was added into DMSO with compound **1** under ultrasonic conditions at 60 °C. Next, the HCFU (2.5 mg, 0.01 mmol) was dissolved into chloroform and dried by a vacuum rotary evaporator (EYELA N-1300). Finally, the DMSO with compound **1** was quickly added into the HCFU and continued ultrasound for 60 min. After cooling, HBS-DDS were successfully prepared. In subsequent studies, the concentration of compound **1** was used to represent the concentration of HBS-DDS.

2.3 Characterization of HBS-DDS

The dynamic light scattering particle size meter (DLS, Zetasizer Nano ZS90, Malvern, UK) was used to measure the hydrodynamic diameter of HBS-DDS. The morphology of HBS-DDS was observed by a transmission electron microscope (TEM, G2F20S-TWIN). Briefly, HBS-DDS was dropped onto the copper mesh and stained with phosphotungstic acid. After drying, the morphology of HBS-DDS was observed by a TEM. The zeta potential of HBS-DDS was measured by a DLS at different pH values. The composition of HBS-DDS was measured by ^{1}HNMR. First, HBS-DDS was cracked using a HCl solution (1 M). Then, the proportions of compound **1** and HCFU were measured by ^{1}HNMR. Finally, the drug loading capacity was calculated as follows: drug loading capacity (wt%) = $(W_{HCFU}/W_{HBS\text{-}DDS}) \times 100\%$.

2.4 Stability assay[17]

The dilution stability was evaluated by measuring the particle size of HBS-DDS with different concentrations (concentration of loaded drug carrier). Briefly, HBS-DDS were diluted to the various concentrations (concentration of loaded drug carrier, 10, 20, 39, 78, 156, 312, 625, 1250, and 2500 μM). Then, the particle sizes of HBS-DDS with different concentrations were

recorded by DLS. The FBS stability of HBS-DDS was tested by co-culturing with 10 v/v% FBS. Then, the particle size of HBS-DDS was determined by DLS at different time periods (0, 1.5, 3, 13, and 24 h).

2.5 Drug release assay[10]

First, HBS-DDS was added to a dialysis bag (2000 Da). Then, the dialysis bag with HBS-DDS was immersed into 100 mL of different buffer solutions (pH 7.4 buffer, 6.5 PBS buffer, and pH 5.5 acetate buffer, 0.1% Tween 80), respectively. Next, the solutions were removed and replaced with fresh buffer solutions at different time points. The content of HCFU released from HBS-DDS was determined by high-performance liquid chromatography (HPLC, HP1100, USA). Detailed condition: column: C18 column; flow rate = 1000 mL min^{-1}; mobile phase was a mixed solution of methanol and water ($V_{methanol}$: V_{water} = 56 : 44); detector absorbance = 258 nm.

2.6 Cellular uptake assay[10]

The cellular uptake behavior of HBS-DDS was examined by confocal laser scanning microscopy (CLSM, Leica Microscopy Systems Ltd, Germany). First, Nile Red was loaded into the core of the HBS-DDS (the detail process was shown in ESI†). Then, the HBS-DDS with Nile-Red were incubated with HeLa cells (DMEM medium containing 10% FBS, Shanghai Institute of cell, Chinese Academy of Sciences) for different time periods. After washing three times with PBS solution, the HeLa cells were fixed with paraformaldehyde for 30 min and stained with Hoechst 33342 for 10 min. Finally, the HeLa cells were observed by a CLSM.

2.7 Antitumor activity and cytotoxicity to normal cells[18,19]

First, the HeLa cells and normal cells (L929 cells, DMEM medium containing 10% FBS, Shanghai Institute of cell, Chinese Academy of Sciences) were seeded in 96-well plates and cultured for 12 h. Then, the old medium was replaced with a fresh medium (100 mL) with various concentrations of HBS-DDS (concentration of loaded HCFU) and HCFU and continued to incubate for 48 h. After co-culturing, the culture medium was replaced with a fresh medium with CCK-8 solution (10 v/v%, 100 μL) and continued to incubate at 37 °C for 2 h. Finally, the optical density (OD) of the solution was measured at 480 nm using a microplate reader (Thermo Fisher Scientific, USA). Finally, the popular calcusyn software was used to calculate the half-maximal inhibitory concentration (IC_{50}) of samples.

2.8 Statistical analysis

Data are presented as the mean ± standard deviation of at least three independent samples, and each measurement was

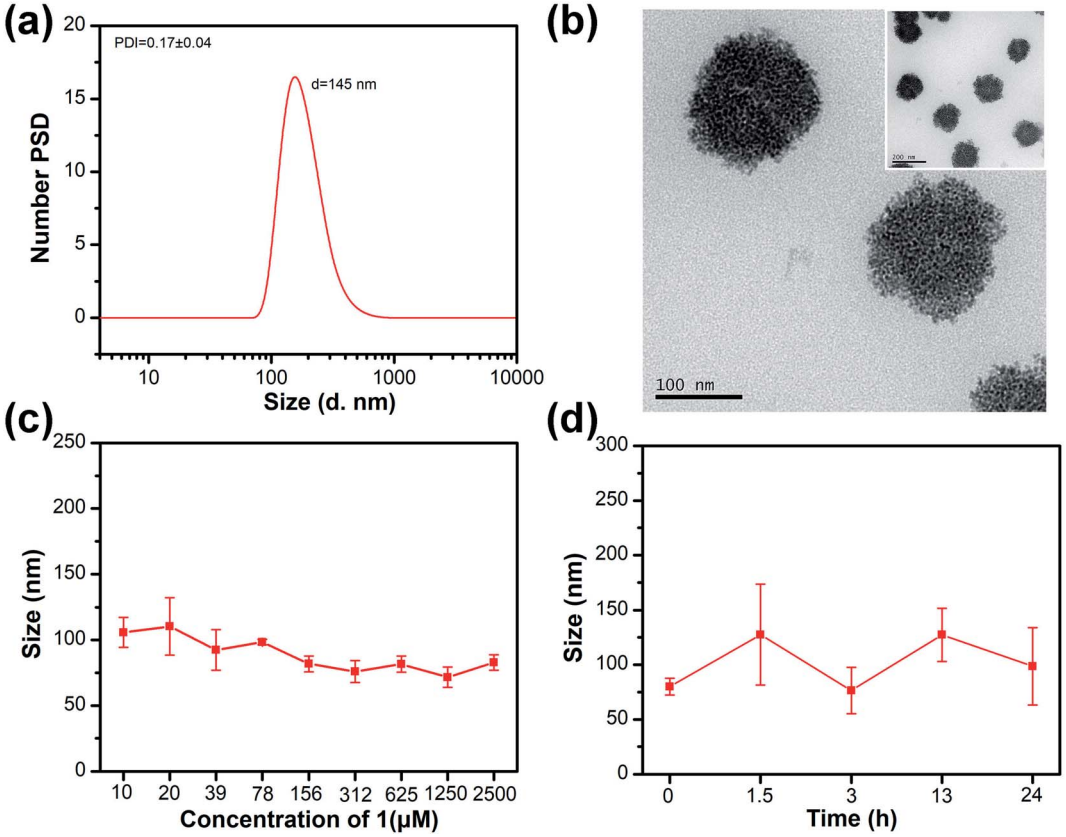

Fig. 1 (a) Distribution of the hydrodynamic diameter of HBS-DDS. (b) TEM images of HBS-DDS. (c) Size of HBS-DDS with various concentrations. (d) Particle sizes of HBS-DDS after incubation with 10% FBS for 24 h. [1] = 5.0×10^{-4} M.

performed in triplicate. Statistical analysis was determined by the analysis of variance tests (ANOVA) using two-tailed, unpaired tests, and the p values < 0.05 were considered to be statistically significant.

3. Results and discussion

3.1 Synthesis and characterization of HBS-DDS

Detailed synthesis steps of the drug carrier (compound **1**) are shown in SI. The ^{1}H NMR, ^{13}C NMR and high-resolution mass spectrum (Fig. S1–S5†) showed that compound **1** was successfully synthesized. The hydrodynamic diameter of HBS-DDS determined by DLS is ~145 nm with unimodal size distribution (Fig. 1a). The polydispersity index (PDI) of HBS-DDS was 0.17 ± 0.04, which indicated that HBS-DDSs displayed a relatively uniform particle size. The TEM images indicated that HBS-DDS presented a spherical morphology (Fig. 1b), which was similar to the size determined by DLS. In order to resist metabolism and then enrich tumor tissue through the EPR effect, high stability was required for drug delivery systems. As shown in Fig. 1c, the particle size did not change significantly, even if HBS-DDS was diluted to the concentration of compound **1** was equal to 10 μM. After incubation in FBS (10%), HBS-DDS showed also a slight size change (Fig. 1d). All these results indicated that the hydrogen bond network endowed HBS-DDS with excellent stability in the normal physiological environment. The drug loading capacity was measured by ^{1}H NMR. As shown in Fig. S6 and Table S1,† the molar ratio of compound **1** to HCFU in HBS-DDS was 1 : 0.94, which was close to the feed molar ratio of 1 : 1, presumably as a result of alternating self-assembly induced by multiple hydrogen bonds between compound **1** and HCFU. Furthermore, the drug loading of HBS-DDS was calculated as 38.1%, which was much more than physical encapsulation and even close to covalent grafting.[20–22] All the above-mentioned results demonstrated that HBS-DDS possessed high drug loading and robust stability, so that it had the potential to become a nano-drug for tumor treatment.

3.2 pH-triggered size change and drug release

As shown in Fig. 2a, the morphology of HBS-DDS was dense with a particle size of 100–150 nm at pH 7.4. The HBS-DDS gradually became loose and dissociated into small nanoparticles with 10–50 nm size at pH 6.5. After pH continues to decrease to 5.5, the small nanoparticle (10–50 nm) was further fluffy and dissociates small fragments. The results indicated that HBS-DDS possessed pH-triggered size change and gradually dissociates into small fragments/nanoparticles with the decrease in the pH value. The size change ability could overcome two intrinsically conflicting (tumor accumulation and penetration) attributes of nano-drugs for tumor treatment.[23] On the one hand, HBS-DDS exhibited a ~100 nm size in the blood (pH 7.4), which was conducive to their enrichment at the tumor site through EPR effect.[24–27] On the other hand, HBS-DDS dissociated into small fragments in the tumor microenvironment (pH 5.5–6.5), so that they could

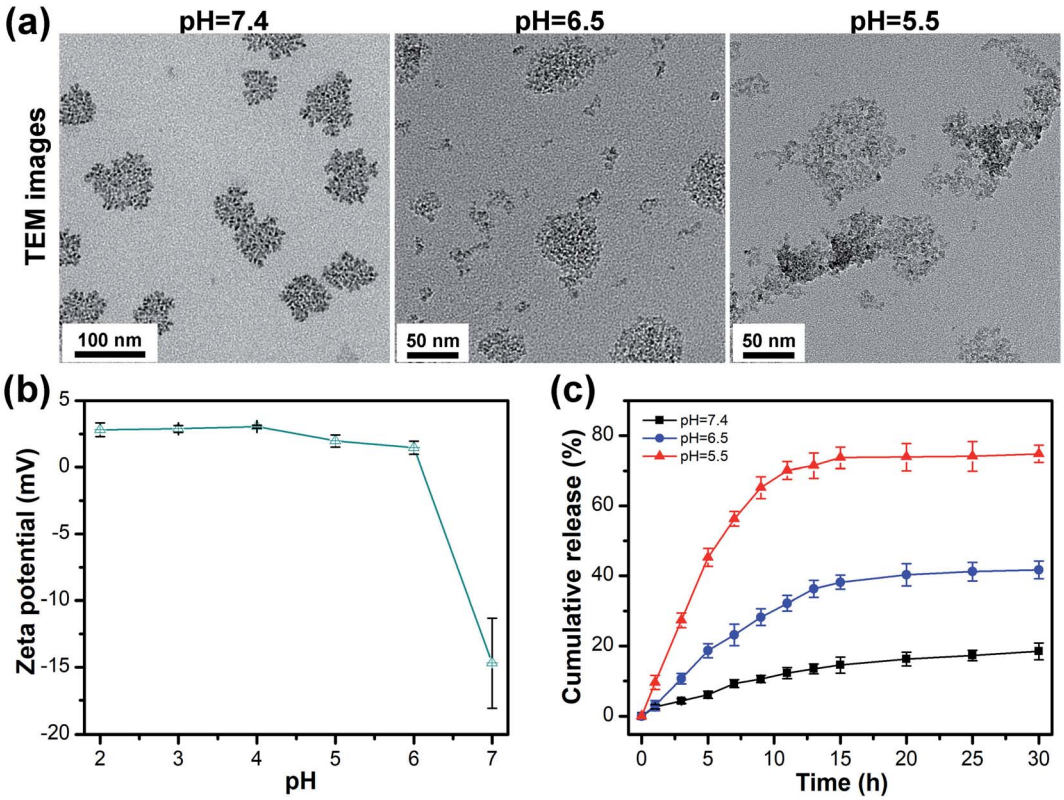

Fig. 2 (a) TEM image of HBS-DDS at different pH values. (b) The zeta potentials of HBS-DDS at different pH values. (c) Time-dependent cumulative release of drug from HBS-DDS at different pH values.

efficiently penetrate the tumor tissue and enter tumor cells. Fig. 2b shows that the zeta potential of HBS-DDS was −14.7 mV at pH 7. However, the zeta potential of HBS-DDS gradually increased with the decrease in pH and was 1.5 mV and 2.0 mV after the pH becomes 6 and 5, respectively. The zeta potential change of HBS-DDS came from the protonation of the amino group in compound **1** after pH reduction, which might cause the weakening of hydrogen bonds (cross-linker of HBS-DDS) between compound **1** and HCFU, thereby leading to HBS-DDS swell and dissociation. As reported, the hydrogen bond could be used for the controlled release of drugs due to its pH sensitivity.[28–31] To test the drug release, HBS-DDS was investigated in a buffer solution with different pH at 37 °C. Fig. 2c reveals the accumulative drug release curve of HCFU from HBS-DDS was markedly correlated with the solution pH values. At neutral pH, the release rate of HCFU was slower from HBS-DDS than pH 6.5 and pH 5.5, and ∼18% HCFU was released from micelles in 30 h at pH 7.4. In contrast, the release of HCFU from HBS-DDS was almost ∼40% and ∼74% at pH 6.5 and 5.5, respectively. These results demonstrate that the release behavior of HCFU from HBS-DDS was pH-dependent, and the lower the pH, the faster the HCFU release rate, as the HBS-DDS would gradually dissociate into fragments after pH decreases. The pH-triggered release behavior of the drug not only avoided the leakage of HCFU in the neutral physiological environment but also enabled HBS-DDS to efficiently release HCFU in the acidic environment of the tumor to achieve efficient anti-tumor. Thus, the pH-triggered release of anticancer drugs was conducive to improving bioavailability and reducing the toxicity of drug.[10,32–34]

3.3 Cell uptake of HBS-DDS

The intracellular uptake of HBS-DDS was evaluated by CLSM after the co-culture of Nile Red-loaded HBS-DDS and HeLa cells

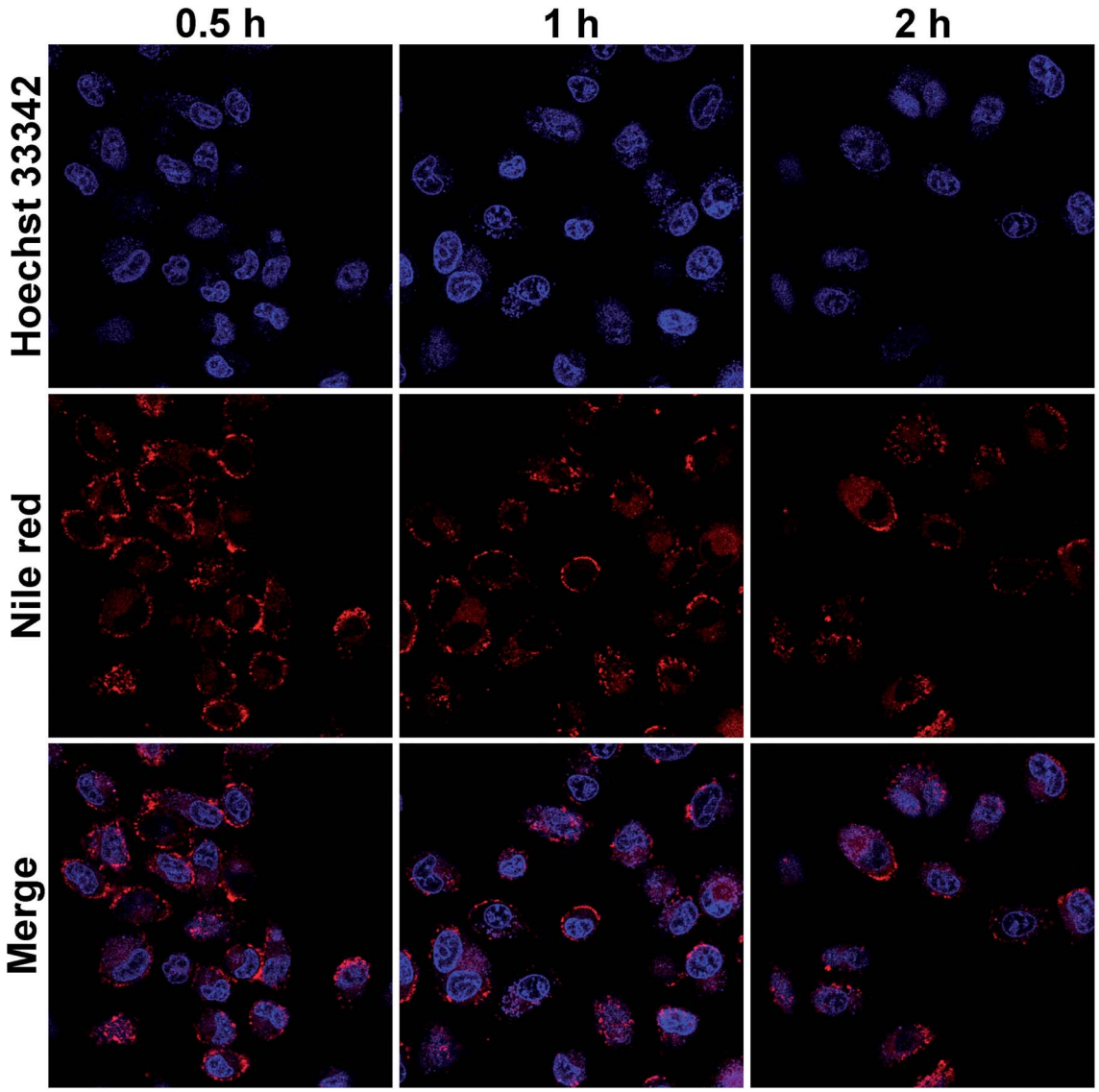

Fig. 3 CLSM images of HeLa cells incubated with Nile Red-loaded HBS-DDS for 0.5, 1, and 2 (blue fluorescence: cell nuclei, red fluorescence: Nile Red, scale bar: 25 μm).

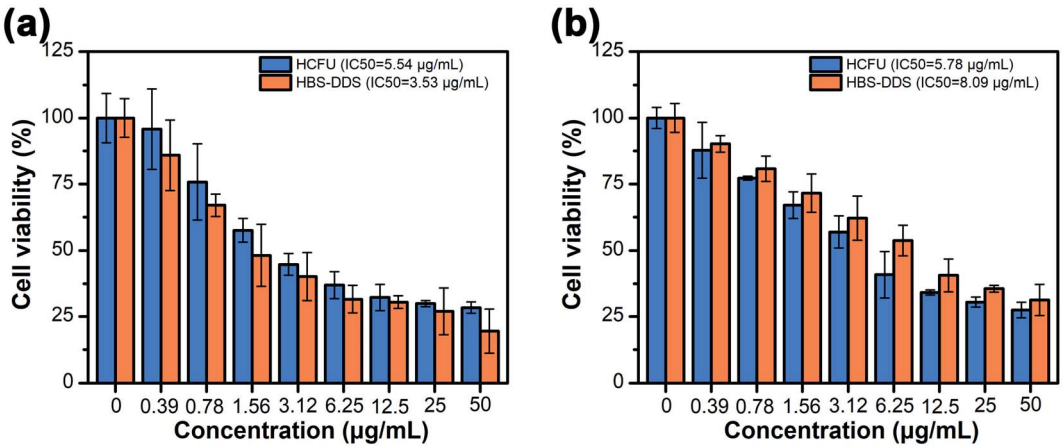

Fig. 4 (a) Cell viability of HCFU and HBS-DDS for HeLa cells after incubation for 48 h. (b) Cell viability of HCFU and HBS-DDS for L929 cells after incubation for 48 h.

(Fig. 3). After co-culture for 0.5 h, a strong red fluorescence (Nile Red) could be observed around the blue fluorescence (cell nucleus), and some of the red fluorescence coincided with the blue fluorescence, suggesting that the Nile Red-loaded HBS-DDS has gradually entered the nucleus. Compared with the co-culture for 0.5 h, the red fluorescence did not significantly increase after co-culture for 1 and 2 h. The result indicated that it took only 0.5 h for a large amount of Nile Red-loaded HBS-DDS to enter the tumor cells through endocytosis. All these results of the intracellular uptake test demonstrated that HBS-DDSs were able to quickly and effectively enter the tumor cells, which was conducive to the efficacy of HCFU.

3.4 Antitumor activity test

The cytotoxicity of carriers (compound **1**) to normal cells (L929 cells) and tumor cells (HeLa cells) should be tested before evaluating the antitumor activity of HBS-DDS. Fig. S9† shows that the cell survival rate was more than 80% of L929 cells and HeLa cells, even if the concentration of compound **1** was as high as 150 μg mL^{-1}. The results demonstrated that compound **1** had good biocompatibility and no obvious anticancer activity. In addition, the anticancer activity of free HCFU and HBS-DDS was evaluated in HeLa cells (Fig. 4). As shown in Fig. 4a, the IC_{50} for the HeLa cells of HBS-DDS (3.53 μg mL^{-1}) was close to that of HCFU (5.54 μg mL^{-1}), suggesting that the HBS-DDS could maintain high anticancer activity similar to that of free HCFU, which was caused due to the following three reasons; (1) the HBS-DDSs were able to quickly and effectively deliver HCFU into tumor cells (Fig. 3); (2) the pH sensitivity of HBS-DDSs (see Fig. 2) avoided the leakage of HCFU in normal environment and the rapid release in tumor cells; (3) compared with covalent grafting, the non-covalent interactions between compound **1** and HCFU did not involve the functional groups of original drugs. The cytotoxicity of the HBS-DDS to normal cells (L929 cells) is shown in Fig. 4b. The IC_{50} for the L929 cells of HCFU was 5.78 μg mL^{-1}, indicating that HCFU exhibited high cytotoxicity for healthy cells as most antitumor drugs were not selective to kill tumor cells and healthy cells.[35,36] By comparison, IC_{50} for L929 cells of HBS-DDSs (8.09 μg mL^{-1}) was higher than that of HCFU, which indicated that the cytotoxicity of HCFU for healthy cells was reduced. The results might be caused by the slow release of HCFU of HBS-DDS due to the neutral environment in normal cells. In short, all the above results demonstrated that the HBS-DDS maintained high anticancer activity of HCFU and reduced its cytotoxicity to normal cells.

4. Conclusions

In summary, the hydrogen-bond super-amphiphile-based drug delivery system has been constructed for tumor therapy under multiple hydrogen bonds between compound **1** and HCFU. The resulting HBS-DDS with a particle size of ~145 nm exhibited a drug loading capacity of up to 38.1%, and the high drug loading capacity ensured the effective delivery of drugs and reduced the number of carriers. In addition, the HBS-DDS could maintain stable particle size even the concentration was diluted to 10 μM or incubated in FBS for 24 h. Thanks to the pH sensitivity of hydrogen bonds, the HBS-DDS exhibited pH-triggered size change and drug release behavior, which was conducive to improving bioavailability and reducing the toxicity of the drug. The anticancer ability test showed that the HBS-DDS could be efficiently ingested by tumor cells and its anticancer efficiency was close to that of free HCFU, indicating that the HBS-DDS maintained original drug activity. Thus, the HBS-DDS with high drug loading capacity, robust stability, original drug activity, and pH responsiveness, and represents a potential drug delivery system in cancer treatment and provides guidance for the design of a new drug loading system.

Conflicts of interest

The authors declare no conflict of interest.

Acknowledgements

This work was supported by grants from the National Natural Science Foundation of China (21975165) and the Innovative

Research Team Program of Sichuan Province (2021JDTD0015). The authors thank the Center of Testing and Analysis, Sichuan University for SEM measurements.

References

1 H. Cabral, K. Miyata, K. Osada and K. Kataoka, *Chem. Rev.*, 2018, **118**, 6844–6892.
2 J. Zhang, C. Li, C. Liao, P. Zhao, Y. Yu and S. Zhang, *Langmuir*, 2019, **35**, 6676–6682.
3 Y. C. Barenholz, *J. Controlled Release*, 2012, **160**, 117–134.
4 C. Liao, Y. Chen, Y. Yao, S. Zhang, Z. Gu and X. Yu, *Chem. Mater.*, 2016, **28**, 7757–7764.
5 B. Peng, P. K. Ang and K. P. Loh, *Nano Today*, 2015, **10**, 128–137.
6 J. Xu, Q. Zhao, Y. Jin and L. Qiu, *Nanomedicine*, 2014, **10**, 349–358.
7 K. J. Chen, L. Tang, M. A. Garcia, H. Wang, L. Hua, W. Y. Lin, S. Hou, Q. Yin, K. F. Shen and J. Cheng, *Biomaterials*, 2012, **33**, 1162–1169.
8 X. L. Hu, S. D. Zhai, G. H. Liu, D. Xing, H. J. Liang and S. Y. Liu, *Adv. Mater.*, 2018, **30**, 1706307.
9 C. G. Palivan, O. Fischer-Onaca, M. Delcea, F. Itel and W. Meier, *Chem. Soc. Rev.*, 2012, **41**, 2800–2823.
10 Y. Chen, J. Huang, S. Zhang and Z. Gu, *Chem. Mater.*, 2017, **29**, 3083–3091.
11 J. E. Zuckerman and M. E. Davis, *Nat. Rev. Drug Discovery*, 2015, **14**, 843–856.
12 J. Boucard, C. Linot, T. Blondy, S. Nedellec, P. Hulin, C. Blanquart, L. Lartigue and E. Ishow, *Small*, 2018, **14**, 1802307.
13 H. Cheng, Y. J. Cheng, S. Bhasin, J. Y. Zhu, X. D. Xu, R. X. Zhuo and X. Z. Zhang, *Chem. Commun.*, 2015, **51**, 6936–6939.
14 B. Nadia, T. N. Axel, W. Christian, N. Toufik, N. Ulrich and L. Andreas, *J. Controlled Release*, 2019, **301**, 146–156.
15 Z. Xu, L. Hu, J. Ming, X. Cui, M. Zhang, J. Dou, W. Zhang and B. Zhou, *Microporous Mesoporous Mater.*, 2020, **303**, 110259.
16 C. C. Cheng, Y. T. Sun, A. W. Lee, S. Y. Huang, W. L. Fan, Y. H. Chiao, C. W. Chiu and J. Y. Lai, *Polym. Chem.*, 2020, **11**, 2791–2798.
17 Y. Yao, X. Dai, Y. Tan, Y. Chen and S. Zhang, *Adv. Healthcare Mater.*, 2021, **10**, 2001430.
18 C. Liao, X. Dai, Y. Chen, J. Liu, Y. Yao and S. Zhang, *Adv. Funct. Mater.*, 2019, **29**, 1806567.
19 X. Gao, M. Wei, D. Ma, X. Yang, Y. Zhang, X. Zhou, L. Li, Y. Deng and W. Yang, *Adv. Funct. Mater.*, 2021, **31**, 2106700.
20 M. Ghorbani, F. Mahmoodzadeh, P. Nezhad-Mokhtari and H. Hamishehkar, *New J. Chem.*, 2018, **42**, 18038–18049.
21 Y. Zhang, C. Y. Ang, M. Li, S. Y. Tan, Q. Qu and Y. Zhao, *ACS Appl. Mater. Interfaces*, 2016, **8**, 6869–6879.
22 Y. Sun, X. Du, J. He, J. Hu, M. Zhang and P. Ni, *J. Mater. Chem. B*, 2017, **5**, 3771–3782.
23 Y. Yao, C. Li, F. Liu, P. Zhao, Z. Gu and S. Zhang, *Phys. Chem. Chem. Phys.*, 2019, **21**, 10477–10487.
24 H. Kang, S. Rho, W. R. Stiles, S. Hu, Y. Baek, D. W. Hwang, S. Kashiwagi, M. S. Kim and H. S. Choi, *Adv. Healthcare Mater.*, 2020, **9**, 1901223.
25 Y. Wang, Z. Wang, C. Xu, H. Tian and X. Chen, *Biomaterials*, 2019, **197**, 284–293.
26 R. Korsmeyer, *Regener. Biomater.*, 2016, **3**, 143–147.
27 H. Xu, B. Ma, J. Jiang, S. Xiao, R. Peng, W. Zhuang, G. Li and Y. Wang, *Regener. Biomater.*, 2016, **3**, 143–147.
28 Z. Xu, L. Hu, J. Ming, X. Cui, M. Zhang, J. Dou, W. Zhang and B. Zhou, *Microporous Mesoporous Mater.*, 2020, **303**, 110259.
29 R. Singh, B. Kumar, R. K. Sahu, S. Kumari, C. B. Jha, N. Singh, R. Mathur and S. T. Hedau, *RSC Adv.*, 2021, **11**, 33723–33733.
30 H. Liang, Y. Pei, J. Li, W. Xiong, Y. He, S. Liu, Y. Li and B. Li, *RSC Adv.*, 2016, **6**, 31374–31385.
31 M. Lin, Y. Dai, F. Xia and X. Zhang, *Mater. Sci. Eng. C*, 2021, **119**, 111626.
32 L. Tan, R. Huang, X. Li, S. Liu, Y.-M. Shen and Z. Shao, *Carbohydr. Polym.*, 2017, **157**, 325–334.
33 Y. Yang, F. Xia, Y. Yang, B. Gong, A. Xie, Y. Shen and M. Zhu, *J. Mater. Chem. B*, 2017, **5**, 8600–8606.
34 S. Chen and R. Chen, *ACS Appl. Mater. Interfaces*, 2016, **8**, 22457–22467.
35 M. H. Lee, A. Sharma, M. J. Chang, J. Lee, S. Son, J. L. Sessler, C. Kang and J. S. Kim, *Chem. Soc. Rev.*, 2018, **47**, 28–52.
36 A. Steinbrueck, A. C. Sedgwick, J. T. Brewster, K. C. Yan, Y. Shang, D. M. Knoll, G. I. Vargas-Zúñiga, X. P. He, H. Tian and J. L. Sessler, *Chem. Soc. Rev.*, 2020, **49**, 3726–3747.